

Heat budget parameters for the southwestern Arabian Sea during Monsoon - 88 experiment

V. RAMESH BABU, V.V. GOPALA KRISHNA and J.S. SASTRY

National Institute of Oceanography, Dona Paula, Goa - 403004, India

Abstract - The temporal evolution of heat budget parameters for the southwestern Arabian Sea shows that the net surface heat balance is negative ($\sim 70 \text{ Wm}^{-2}$) in May 1988 (phase 1) mainly due to excessive latent heat loss over the radiation income while during August-September 1988 (phase 2), it has become positive on account of decrease in evaporative heat flux by about 25 % of the phase 1 value ($\sim 240 \text{ Wm}^{-2}$). The lowering of specific humidity gradient by 1.5 from phase 1 to phase 2 is mainly responsible for lower evaporation rates during the latter period. The monsoonal cooling, ($\sim -87 \text{ Wm}^{-2}$) effects confine to upper 100 m layer and the heat gain at an average rate of about 160 Wm^{-2} is noticed below upto 500 m depth. The cooling in the upper layers is partly accounted by the surface heat exchange processes and the subsurface heat gain suggests the influence of sinking motion in the study area wherein the dynamic topography field is predominantly characterised with clockwise circulation.

INTRODUCTION

Monsoon-88 experiment was conducted over the southwestern Arabian Sea under a joint Indo-Soviet programme in oceanography from March to September, 1988 covering pre-onset, onset and post-onset phases of summer monsoon in order to understand the evolution of air-sea interactive processes and the development of ocean circulation patterns. Some of the meteorological results pertaining to pre-onset phase (March-April) of the Monsoon-88 were earlier presented by SADHURAM *et al* (1989). The north-south XBT sections in the southwestern Arabian Sea during summer monsoon have indicated a trough in the thermocline whose intensity is related to the strength of southwest monsoon (RIVERDIN and FIEUX, 1987). Most of the intra-seasonal studies of the western Arabian Sea have addressed the temporal variability in the flow patterns. The time scale involved in the oceanic response to the summer monsoonal wind forcing is of about a month (SWALLOW *et al*, 1983). The evolution of thermal structure of the Arabian Sea is chiefly characterised with a pronounced surface cooling on account of coastal upwelling (DÜING and LEETMAA, 1980) in spite of net heat gain from the atmosphere (HASTENRATH and LAMB, 1979b).

Thermal modifications in the ocean may have a feed-back effect on the monsoon rainfall on different time scales and the southwestern Arabian Sea is considered as one of the energy active zones for the summer monsoon. Strong positive (negative) correlations exist between the premonsoonal (postmonsoonal) sea surface temperature fields and the summer monsoon rainfall over India (WU and HASTENRATH, 1986 ; SHUKLA, 1987). The annual and seasonal heat budget studies of the Indian Ocean indicate the importance of the upwelling in the Arabian Sea in maintaining the steady state conditions (HASTENRATH and LAMB, 1980). In this paper, the heat budget of the southwestern Arabian Sea is examined using surface meteorological and the hydrographic data of the Monsoon-88 collected during May (phase 1) and August-September (phase 2) representing pre-onset and post-onset conditions of summer monsoon respectively with reference to rainfall pattern over India. During 1988, the summer monsoon had set in over Kerala towards the end of May and covered the peninsula, Gujarat and northeast India by 14 June. It covered central parts of India by 17 June

and the entire country by 1 July. The activity of monsoon in 1988 for the country as a whole was above normal (departure: $> + 20\%$) during July-September. The monsoon had begun withdrawing from 12 September over north India and it had fully withdrawn from the country by 15 October.

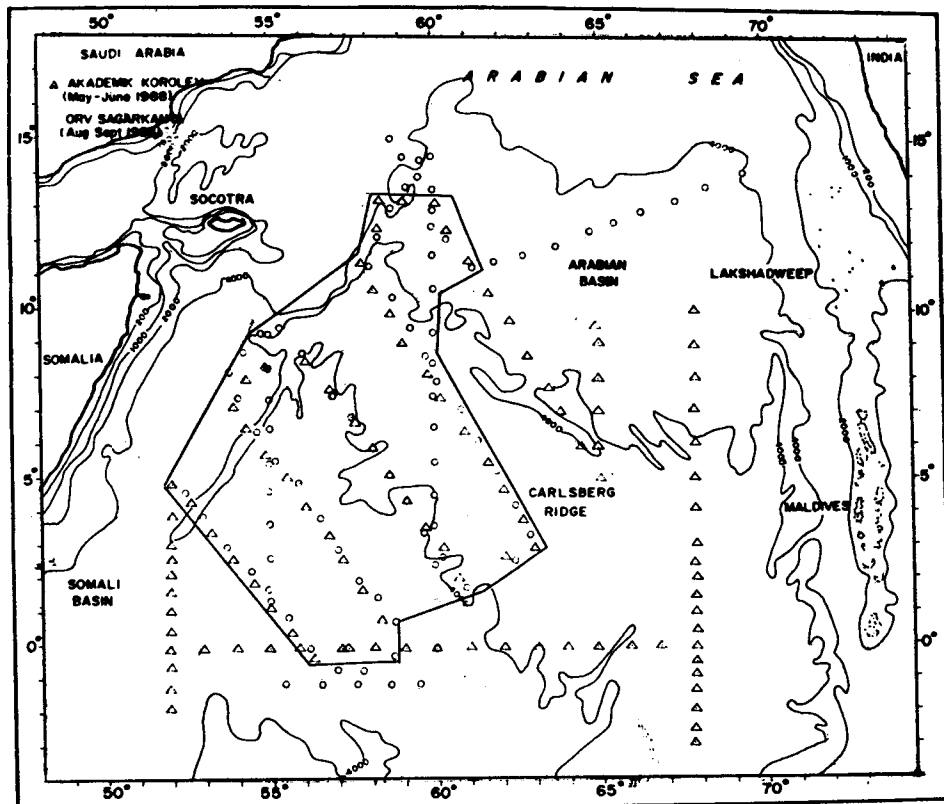


Fig. 1. Study area with the locations of hydrographic stations during Monsoon-88 experiment. Part of this area is marked as a polygon to compute area averages for the stations occupied during both the phases.

DATA AND METHODS

Fig. 1 shows the locations of hydrographic and XBT stations in the southwestern Arabian Sea during the phase 1 and phase 2 regimes of the summer monsoon, 1988. The research ship, *RV Akademik Korolev* of USSR hydrometeorological service had surveyed the area during the pre-onset period (May-June, 1988) and collected 93 XBT profiles. The same area was resurveyed during post-monsoon period (August-September, 1988) by the Indian research ship *ORV Sagarkanya* occupying 105 hydrographic stations. The surface meteorological data were collected at three hourly interval during both the cruises. Table 1 gives out the details of these cruises organised as part of Monsoon-88 experiment. Various individual surface heat flux parameters computed at each observed time were averaged on daily basis for the spatial analysis. The uncertainties in the estimates of various surface fluxes through empirical and bulk aerodynamic formulae are stated to be within twenty percent of their true values (HASTENRATH and LAMB, 1979 b). These average estimates based on the observations spread over an area covered during 24 hrs have a bias possibly due to spatial gradients

and temporal variations as discussed by WEARE and STRUB (1981). However, the total bias on account of all these uncertainties is believed to be within the 10% accuracy limit since the study area is adequately sampled to meet the threshold requirement of minimum 11 observations per 5° square for arriving at more accurate estimates. The total number of surface meteorological observations taken in the study area comprising twelve five degree grids are 191 and 328 for pre-onset and post-onset monsoon periods respectively.

The methodology of STEVENSON (1982) was adopted to compute the heat fluxes at sea surface after reducing the meteorological data collected at different heights of 22 m (ORV AKADEMIK KOROLEV) and 19 m (ORV SAGARKANYA) to a standard anemometer height (10 m). The net surface heat flux Q_N (Wm^{-2}) is given by

$$Q_N = Q_I (1-\alpha) - Q_B - Q_E - Q_S$$

where Q_I is the short wave radiation incident at the sea surface, α is the albedo, Q_B is the effective back radiation and Q_E & Q_S are the latent and sensible heat fluxes.

Table 1. Oceanographic cruises organised as a part of Monsoon-88 experiment

| Ship name | Cruise No. | Duration (days) | Starting date | Ending date | No. of stations occupied |
|------------------|------------|-----------------|---------------|----------------|--------------------------|
| Akademik Korolev | 46B | 26 | May 6, 1988 | May 31, 1988 | 93 |
| Sagar Kanya | 43 | 41 | Aug 3, 1988 | Sept. 12, 1988 | 105 |

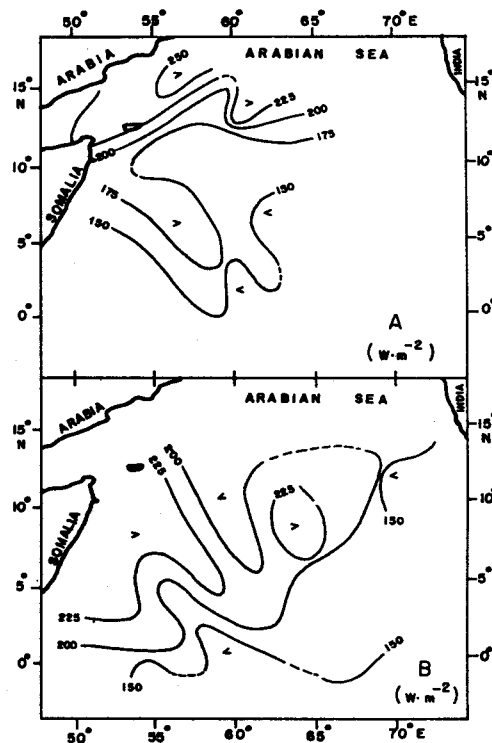
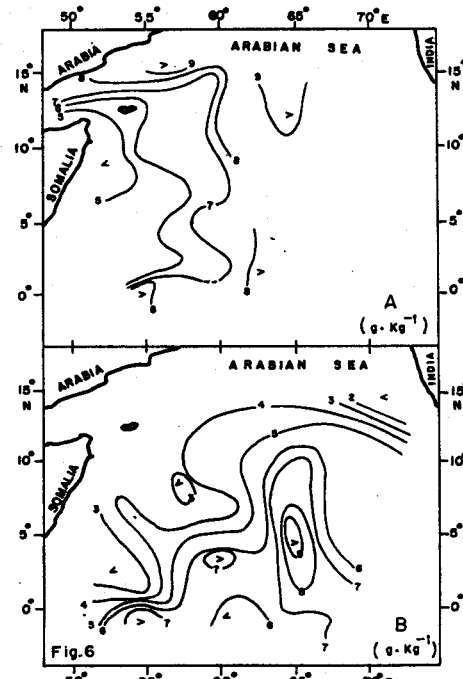
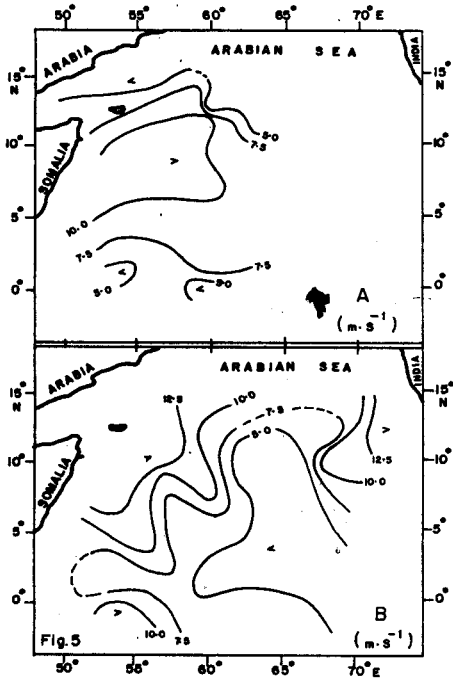
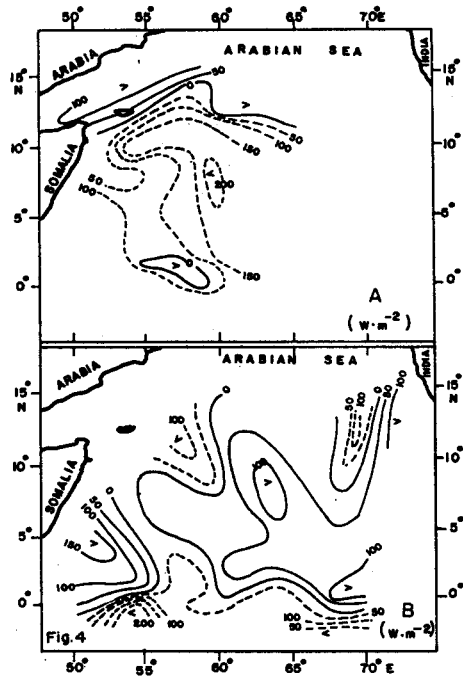
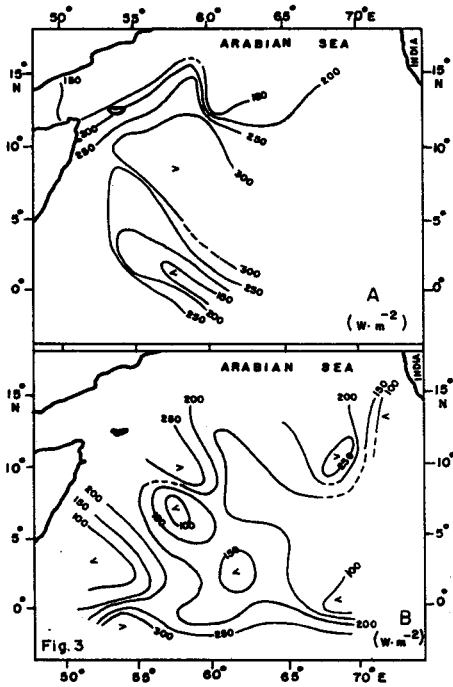


Fig. 2. Net radiation (Wm^{-2}) during (A) May, 1988 (phase 1) and (B) August-September (phase 2) periods of Monsoon-88 experiment.



Figs. 3 - 6. Evaporative heat flux (Wm^{-2}), Net surface heat flux (Wm^{-2}), Surface wind speed (ms^{-1}) and Specific humidity gradient $q_s - q_{10}$ (gKg^{-1}) respectively during (A) May, 1988 (phase 1) and (B) August-September (phase 2) periods of Monsoon-88 experiment.

The heat content H (Jm^{-2}) in the water column is computed according to equation:

$$H = \rho_w C_{pw} \int_0^z T \, dz$$

where ρ_w is the density of sea water (1000 Kg m^{-3}) and C_{pw} is the specific heat capacity of water ($3.94 \text{ Joules g}^{-1} \text{ }^\circ\text{C}^{-1}$) at constant pressure and Z is the vertical coordinate with positive downward.

RESULTS

Fig. 2 shows the distribution of net radiation ($Q_I - Q_B$) during phase 1 and phase 2. The net radiation in general increased from south to north during phase 1 and towards northwest during phase 2. The net radiation increased off Somalia from phase 1 to phase 2. During phase 1, a region of high latent heat flux ($>300 \text{ Wm}^{-2}$) sandwiched between two areas of lower flux ($<150 \text{ Wm}^{-2}$) on the northern and southern sides was noticed between 5°N and 10°N (fig.3A). On the other hand, the distribution of Q_E was completely reversed during phase 2 with the incidence of a well extended area of minimum flux ($<150 \text{ Wm}^{-2}$) centered around 3°N (Fig.3B). On the whole, the average value of Q_E for the polygon area (marked in Fig.1) wherein the stations were occupied during both cruises was decreased by about 25% from that ($\sim 240 \text{ Wm}^{-2}$) of the pre-onset regime (Table 2).

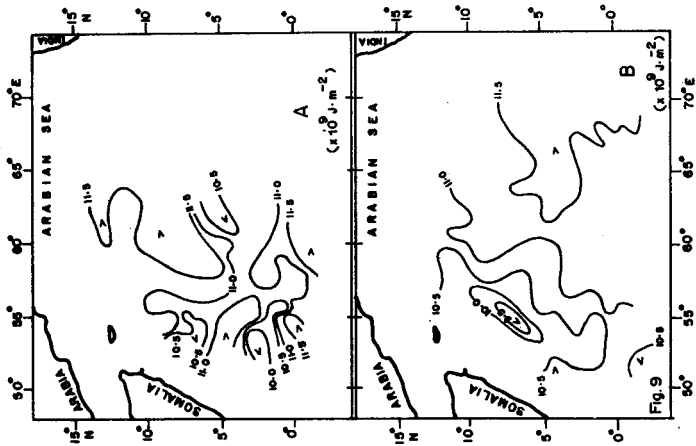
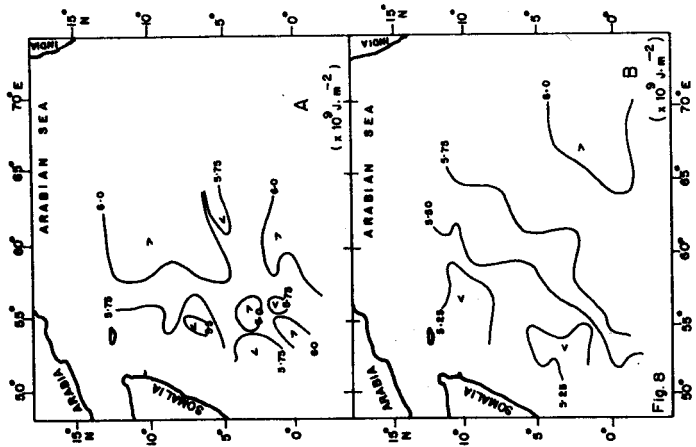
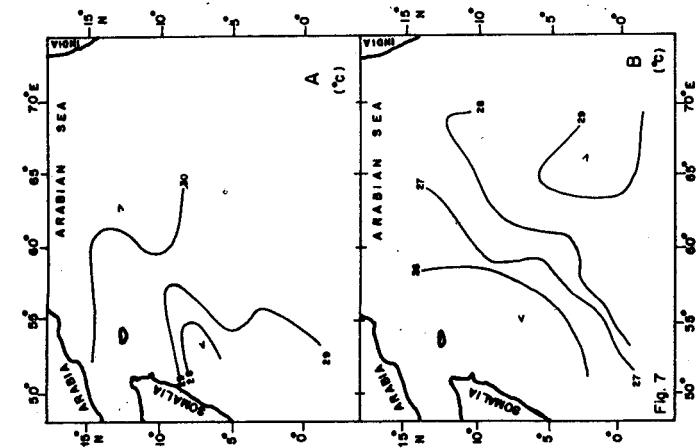
Table 2a. Polygon area averages of surface heat flux, wind and humidity gradient parameters during phases 1 and 2.

| Parameters | Units | Phase 1 | Phase 2 |
|-------------|-------------------|---------|---------|
| Q_I | Wm^{-2} | 219 | 256 |
| Q_I (1-) | Wm^{-2} | 206 | 241 |
| Q_B | Wm^{-2} | 33 | 38 |
| Q_E | Wm^{-2} | 242 | 178 |
| Q_s | Wm^{-2} | 7 | 7 |
| Q_N | Wm^{-2} | -76 | +18 |
| $q_e - q_a$ | gKg^{-1} | 6.5 | 5.0 |
| W_{10} | ms^{-1} | 8.0 | 6.4 |

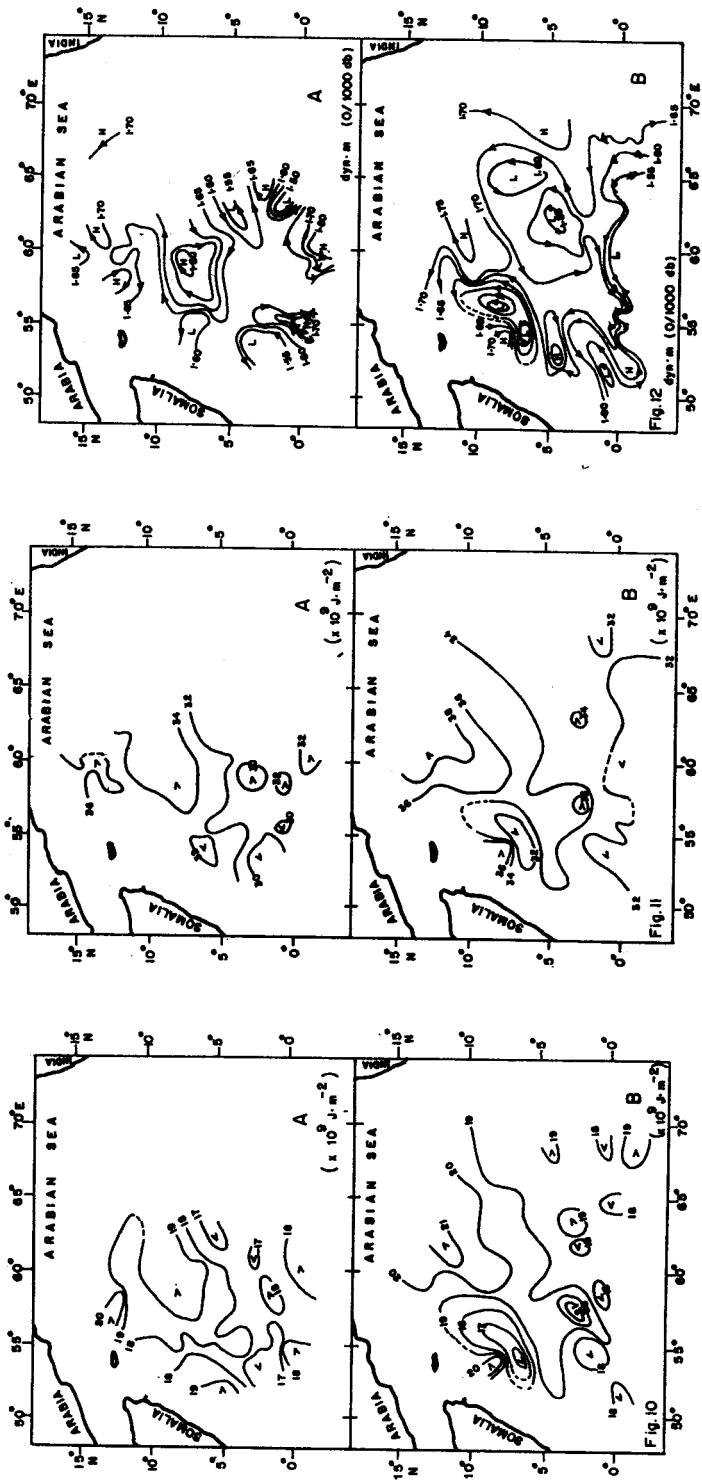
Table 2b. Polygon area averages of heat storage in different layers

| | 0-50 m | 50-100 m | 100-200 m | 200-500 m |
|--|--------|----------|-----------|-----------|
| Phase 1 ($\times 10^9 \text{ Jm}^{-2}$) | 6.04 | 5.49 | 7.39 | 14.30 |
| Phase 2 ($\times 10^9 \text{ Jm}^{-2}$) | 5.51 | 5.26 | 8.02 | 15.06 |
| Seasonal heat content change ($\times 10^9 \text{ Jm}^{-2}$) | -0.53 | -0.23 | +0.63 | +0.76 |
| Rate of heat storage (Wm^{-2}) | -60.74 | -26.36 | +72.19 | +87.09 |

Fig.4 presents the spatial variation of the net surface heat transfer (Q_N). Almost the entire study area south of 12°N was encountered a higher net surface heat loss upto about 200 Wm^{-2} during phase 1. The same area except the equatorial part gained heat from the atmosphere during phase 2. This pattern reflects the dominant role of Q_E in determining Q_N . The decrease in Q_E and the corresponding increase in Q_N in phase 2 over major portion of the southwestern Arabian Sea are the noteworthy results of the present study.



Figs. 7 - 9. Sea surface temperature ($^{\circ}\text{C}$), Heat storage in 0-50 m layer ($\times 10^9 \text{ J m}^{-2}$) and Heat storage in 0-100 m layer ($\times 10^9 \text{ J m}^{-2}$) respectively during (A) May, 1988 (phase 1) and (B) August-September (phase 2) periods of Monsoon-88 experiment.



Figs. 10 - 12. Heat storage in 0-200 m layer ($\times 10^9 \text{ J m}^{-2}$), Heat storage in 0-500 m layer ($\times 10^9 \text{ J m}^{-2}$) and Sea surface dynamic topography field (dyn.m) with reference to 1000 db during (A) May, 1988 (phase 1) and (B) August-September (phase 2) periods of Monsoon-88 experiment.

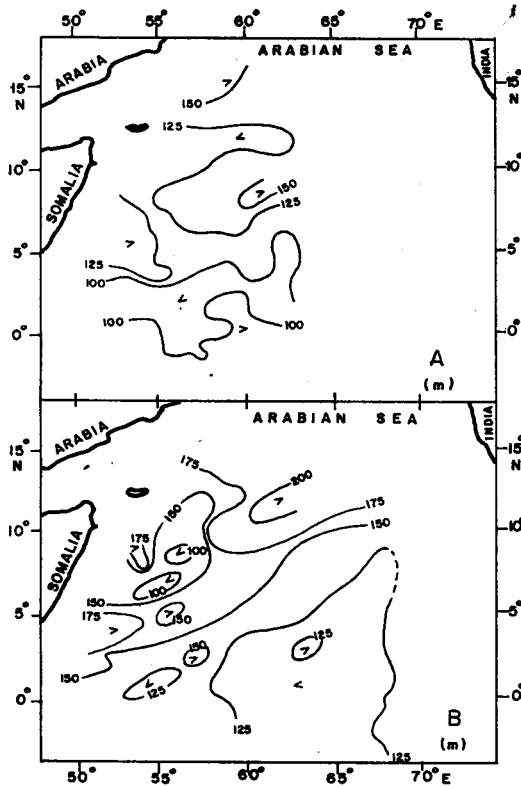


Fig. 13. The depth of 20°C isotherm (m) during (A) May, 1988 (phase 1) and (B) August-September (phase 2) periods of Monsoon-88 experiment.

The relative roles of wind speed and specific humidity gradient on Q_E are assessed through the examination of their spatial patterns as presented in Figs. 5 and 6 respectively. The surface wind distribution (Fig.5) depicts the onset of the monsoon limited to the southern Arabian Sea only as seen from the axis of wind maximum ($>7.5 \text{ ms}^{-1}$) around 8°N during phase 1 which has been earlier represented as the pre-onset period in relation to rainfall pattern over the India. On the other hand, its post-onset characteristic over the central Arabian Sea and the neighbouring west coast of India was typically marked by the clockwise rotation from west to east in the axis of wind maximum ($>10 \text{ ms}^{-1}$). Winds were strengthened west of 55°E while in the southeastern part of the study area they were found to be less than 5 ms^{-1} in phase 2 indicating a larger airmass transport from the southern hemisphere across the western equatorial part of the Indian Ocean. These simultaneous strengthening and weakening in the surface wind field in the northwestern and southeastern parts of the study area respectively from phase 1 to phase 2 are responsible for keeping the polygon area average (W_{10}) value relatively steady (Table 2). The specific humidity gradient (Fig.6) was in general high during phase 1 with values ranging from 5 to 9 gKg^{-1} whereas the spatial range was moderately increased in phase 2 on account of occurrence of much lower values ($<3 \text{ gKg}^{-1}$) along the axis of surface wind maximum. The post-onset distribution of $q_s - q_{10}$ was largely determined by the sea surface temperature (Fig.7) as seen from the coincidence of low and high specific humidity gradients with the corresponding values of sea surface temperature. Maximum cooling of the sea surface in response to the onset of summer

monsoon was observed towards the Somalia coast whereas the central equatorial Indian Ocean was less cooled.

The contribution of surface heat fluxes on heat content changes in the water column of 0-500 m has been assessed. Figs.8 to 11 present the distributions of heat stored in different layers viz., 0-50, 0-100, 0-200 and 0-500 m respectively. During phase 1, the pattern of heat storage in upper 50 m (Fig.8) was relatively complex with the occurrence of several isolated pockets of cold and warm waters in contrast to a better organised pattern one of phase 2. In general, the heat content was reduced from phase 1 to phase 2 on account of the removal of heat by the atmospheric processes during the monsoon season. A decreasing gradient towards Somalia coast was noticed during phase 2 due to upwelling of cold waters. The heat storage in 0-100 m layer (Fig.9) showed a similar distribution with a pronounced decrease towards the Somalia coast. Further, the average heat content decrease in 50-100 m of the polygon area from phase 1 to phase 2 was reduced by about half of that in 0-50 m layer (Table 2b). The subsurface warming occurred below 100 m depth with the onset of the summer monsoon as seen from the increase in the content of 100-200 m layer by $0.63 \times 10^9 \text{ Jm}^2$ from phase 1 to phase 2. The influence of surface exchange processes was no more felt below 100 m depth since the distribution of heat stored in upper 200 m (Fig.10) was not similar to the sea surface temperature pattern. In general, the warm waters were noticed north of 6°N as well as in the equatorial regions separated by a cold area around 3°N . In the polygon area, the heat content in upper 500 m was increased by about $0.60 \times 10^9 \text{ Jm}^2$ from phase 1 to phase 2 suggesting the downward penetration of subsurface warming. The rate of subsurface warming was around 160 Wm^{-2} in 100-500 m layer of the polygon area (Table 2b). The extension of subsurface warming to greater depths upto 500 m is clearly visualised in Fig. 11 wherein the isopleth of $34 \times 10^9 \text{ Jm}^2$ covers about 50 % of the study area during phase 2. The general rise in heat content in upper 500 m of the study area works out to be 72 Wm^{-2} (Table 2b) which masks the near surface cooling event occurring at a rate of -87 Wm^{-2} in upper 100 m. The air-sea heat exchange processes result in a time average of net surface heat loss to the atmosphere over the polygon area by 30 Wm^{-2} (Table 2a) which accounts nearly 50% of upper layer (0-50 m) cooling. The sub-surface warming below 100 m seems to be the result of the circulation patterns in the area determining the convergence or the divergence of the heat into or away from the water body.

The surface dynamic topography field with reference to 1000 db pressure surface during phase 1 (Fig. 12A) was predominantly characterised with a clockwise circulation cell in the central portion of the study area surrounded by several small-scale anticlockwise cells. On the other hand, during phase 2, the circulation was mainly dominated by peripheral cyclonic cells rather than by the central anticyclonic cell as seen from the intensification and spreading of the anticlockwise rotation cells (fig.12B). These modifications would limit the lowering of the thermocline due to typical negative windstress curl of the study area (HELLERMAN and ROSENSTEIN, 1983). On an average, the depth of thermocline as represented by the topography of 20°C isotherm in the study area was deepened moderately from phase 1 to phase 2 as seen from Fig. 13. The polygon area averages for phase 1 and phase 2 were worked out to be 116 and 179 m respectively.

DISCUSSION

The observed seasonal downwelling rate 'w' has been estimated at $0.72 \times 10^{-5} \text{ ms}^{-1}$ in the polygon area after considering the increase in the depth of 20°C isotherm within a time interval of 101 days and the thermocline lowering in association with an increase in temperature further causes subsurface warming. The heat transport Q_{dw}

due to downwelling is computed by the eq: $Q_{dw} = \rho_w C_p w \Delta T$ (DÜING and LEETMAA, 1980) where ΔT is the temperature change due to thermocline deepening. ΔT was 5°C as estimated from the average increase in the temperature at 116 m in the area of study from phase 1 to phase 2. Q_{dw} is estimated at 155 Wm^{-2} which is very close to the observed increase in the heat content of the water column of 100-500 m (table 2b). The seasonal wind stress curl values based on climatological data of HELLERMAN and ROSENSTEIN (1983) as well as on the satellite scatterometer data (CHELTON et al., 1990) should normally give rise to higher downwelling (Ekman pumping) rate of about $1.0 \times 10^{-5} \text{ ms}^{-1}$. However, the present low estimate of actual downwelling rate of $0.72 \times 10^{-5} \text{ ms}^{-1}$ which is about 30% less than the normal Ekman pumping rate suggests the role of dynamic topography in limiting the thermocline deepening. The influence of wind is perhaps felt initially at the time of the monsoon onset when the thermocline is shallow. The studies of GOPALAKRISHNA et al (1988) have earlier indicated that the mixed layer development is more dependent on the initial value of the mixed layer thickness itself and a shallow thermocline responds better to the wind forcing. Further, the non-coincidence of the regions of the maximum Ekman pumping with those of the maximum mixed layer depth during monsoon season (NAIDU and RAO, 1990) indicates the important role of the other forces on the mixed layer development in the southern Arabian Sea. The present study shows that the subsurface warming is accounted due to downwelling processes. However after local heat storage, the convergence of heat due to sinking processes is to be compensated by horizontal advective processes in order to achieve steady state conditions. This is confirmity with the studies of SHETYE (1986) in which the simulation of sea surface temperature on seasonal cycle in a zonal strip around 10° N in the Arabian Sea has been found better when the influence of the advection is considered.

Acknowledgements - We wish to express thanks to Dr B N DESAI, Director of NIO, for his interest in the present study conducted as a part of Indo-USSR bilateral programme in physical oceanography. We also appreciate the cooperation given by the chiefs of the expeditions, cruise participants, respective captains and crew members of both RV *AKADEMIK KOROLEV* and ORV *SAGAR KANYA* during the field programme.

REFERENCES

- CHELTON D.B., A.M.MESTY-NUNEZ and M.H. FRELICH (1990) Global wind stress and Sverdrup circulation from seasat scatterometer. *Journal of Physical Oceanography*, 20, 1175-1205.
- DÜING W and A.LEETMAA (1980) Arabian Sea cooling : A preliminary heat budget. *Journal of Physical Oceanography*, 10, 307- 312.
- GOPALAKRISHNA V.V., Y.SADHURAM and V.RAMESH BABU (1988) Variability of mixed layer depth in the northern Indian Ocean during 1977 and 1979 summer monsoon seasons. *Indian Journal of Marine Sciences*, 17, 258-264.
- HASTERNRATH S and P.LAMB (1979a) *Climatic Atlas of the Indian Ocean. Part-1 : Surface Circulation and Climate*, University of Wisconsin Press, Madison, 104 pp.
- HASTERNRATH S and P.LAMB (1979b) *Climatic Atlas of the Indian Ocean. Part-2 : The Oceanic heat budget*, University of Wisconsin Press, Madison, 14 pp.
- HASTERNRATH S and P.LAMB (1980) On the heat budget of hydrosphere and atmosphere in the Indian Ocean. *Journal of Physical Oceanography*, 10, 694-708.
- HELLERMAN S and M.ROSENSTEIN (1983) Normal monthly wind stress over the world ocean with error estimates. *Journal of Physical Oceanography*, 13, 1093-1104.
- NAIDU V.S and G.R.L.RAO (1990) Ekman pumping velocity and the depth of mixed layer of the north Indian Ocean during southwest monsoon. *Indian Journal of Marine Sciences*, 19, 257-260.
- RIVERDIN G and M.FIEUX (1987) Sections in the western Indian Ocean - Variability in the thermal structure. *Deep-Sea Research*, 34, 601-626.
- SADHURAM Y., L.KRISHNAMURTHY and M.T.BABU (1989) Meteorological results of Monsoon-88 expedition (pre-monsoon period). *Boundary-Layer Meteorology*, 48, 333-344.
- SHETYE S.R (1986) A model study of the seasonal cycle of the Arabian Sea surface temperature. *Journal of Marine Research*, 44, 521-540.

- SHUKLA J. (1987) Intra-annual variability of monsoons. In: *Monsoons*, J.S. FEIN and P.L.STEPHENS, editors, Willy, Newyork, pp.399-463.
- STEVENSON J.W.(1982) Computations of heat and moisture fluxes at the sea surface during the Hawaii to Tahati shuttle experiment. *Technical report No.82-0044*, JIMAR, University of Hawaii, Hanolulu, 27 pp.
- SWALLOW J., R.MOLINARI, J.BRUCE, O.BROWN and R.EVANS(1983) Development of near surface flow pattern and watermass distribution in the Somali basin in response to the southwest monsoon of 1979. *Journal of Physical Oceanography*, 3, 1398-1415.
- WEARE B.C and P.T.STRUB (1981) The significance of sampling biases on calculated monthly mean oceanic surface heat fluxes. *Tellus*, 33, 211-224.
- WU M.C and S.HASTERNRATH (1986) On the intra-annual variability of the Indian monsoon and the southern oscillation. *Archives for Meteorology, Geophysics and Bioclimatology, Series B* , 36, 239-262.